Branching Ratio for the Self-Reaction of Acetonyl Peroxy Radicals

Martin Emrich[a] and Peter Warneck

Max-Planck-Institut für Chemie, D-55020 Mainz, Germany
[a] Saarberg-Interplan, D-66115 Saarbrücken, Germany

Reprint requests to Prof. P. W.: E-mail: biogeo@mpch-mainz.mpg.de

Z. Naturforsch. **58a,** 429 – 433 (2003); received April 24, 2003

Mixtures in air of chlorine, acetone, nitrogen dioxide, and nitric oxide (partly) were photolysed at 330 nm wavelength to produce acetonyl peroxy radicals and to determine the fraction of acetonoxy radicals formed in one of the two branches of the self-reaction of acetonyl peroxy, $2CH_3COCH_2OO\cdot \rightarrow CH_3COCHO + CH_3COCH_2OH + O_2$ (3a) and $2CH_3COCH_2OO\cdot \rightarrow 2CH_3COCH_3O\cdot + O_2$ (3b). In these experiments the decomposition of acetonoxy gives rise to acetyl peroxy radicals, which react with NO_2 to form peroxy acetyl nitrate (PAN). The quantum yield of PAN was measured as a function of time. Computer simulations were used to explore the effect of acetonyl peroxy nitrate as an unstable intermediate formed in the reaction $CH_3COCH_2OO\cdot + NO_2 \rightleftharpoons CH_3COCH_2OONO_2$ (9). The experimental data were evaluated to derive for the rate coefficients associated with reaction (3) the branching ratio $k_{3b}/(k_{3a} + k_{3b}) = 0.50 \pm 0.05$ and for the reverse path of reaction (9) the rate coefficient $k_{-9} = 10.0 \pm 3\ s^{-1}$.

Key words: Acetonyl Peroxy; Peroxy Radical; Self-Reaction Branching Ratio; Acetonyl Peroxy Nitrate.

1. Introduction

The acetonyl peroxy radical can be produced by reacting chlorine atoms with acetone in the presence of oxygen:

$$Cl + CH_3COCH_3 \rightarrow HCl + CH_3CO\dot{C}H_2, \quad (1)$$

$$CH_3CO\dot{C}H_2 + O_2 \rightarrow CH_3COCH_2OO\cdot. \quad (2)$$

Like other organic peroxy radicals, the acetonyl peroxy radical reacts with itself along two major pathways:

$$2\,CH_3COCH_2OO\cdot \rightarrow CH_3COCH_2OH + CH_3COCHO + O_2, \quad (3a)$$

$$\rightarrow 2CH_3COCH_2O\cdot + O_2. \quad (3b)$$

One branch leads to hydroxyacetone and methylglyoxal as stable products, the other branch produces acetonoxy radicals. The overall rate coefficient for reaction (3) is known from two studies with concordant results [1,2], $k_3 = (8 \pm 2) \times 10^{-12}$ cm^{-3} $molecule^{-1}$ s^{-1}. The techniques used were pulse radiolysis of SF_6 and flash photolysis of Cl_2 in the presence of acetone and oxygen. Bridier *et al.* [2] also derived the branching ratio $k_{3b}/k_3 = 0.75 \pm 0.1$ from a kinetic analysis of the time-dependent optical absorption of peroxy radicals at several wavelengths in the near ultraviolet spectral region. The acetonoxy radical is known to undergo rapid decomposition [3,4], whereas the parallel reaction (4) with oxygen

$$CH_3COCH_2O\cdot + O_2 \rightarrow CH_3COCHO + HO_2, \quad (4)$$

$$CH_3COCH_2O\cdot \rightarrow CH_3\dot{C}O + HCHO, \quad (5)$$

$$CH_3\dot{C}O + O_2 \rightarrow CH_3C(O)OO. \quad (6)$$

is unimportant in comparison. The acetyl radical formed in reaction (5) is rapidly converted to acetyl peroxy, which then reacts with other peroxy radicals in the system to form methyl peroxy, methoxy and hydroperoxy radicals. The product distribution resulting from the interaction of all the species in the system is complex [3]. Moreover, all peroxy radicals exhibit ultraviolet absorption features, so that Bridier *et al.* [2] had to apply computer simulations to disentangle the individual contributions to the total signal. The complexity of the system may be the main reason why to our knowledge the branching ratio of reaction (3) has not been reinvestigated.

In previous studies of the photolysis of acetone [5,6] it has been possible to simplify the system by adding nitrogen dioxide as a scavenger for acetyl peroxy radicals and to determine their yield from that of peroxyacetyl nitrate (PAN) formed in the reaction

$$CH_3C(O)OO\cdot + NO_2 \rightleftharpoons CH_3C(O)OONO_2. \quad (7)$$

At 25 °C, the thermal decomposition of PAN is slow, so that it may be ignored on the time scale of the experiments. We have used this technique to reinvestigate the self-reaction of acetonyl peroxy radicals. It was expected that the addition of NO_2 to the system would suppress subsequent reactions of acetyl peroxy radicals, which would enable us to determine the branching ratio of reaction (3) directly from the yield of PAN. Trial experiments showed that appreciable amounts of PAN were indeed formed, when acetonyl peroxy radicals were generated by reactions (1) and (2) in the presence of NO_2, using the photolysis of molecular chlorine as source of chlorine atoms. However, a closer inspection of other reactions in the system revealed that two processes may give rise to detrimental side effects. One is the photolysis of NO_2. The products NO and O may interfere either directly or indirectly with processes involving acetonyl peroxy radicals, so that the yield of PAN is not solely determined by the branching ratio of reaction (3). The second effect is the temporary storage of acetonyl peroxy radicals in the form of acetonyl peroxy nitrate [7], a thermally unstable compound resulting from the addition of NO_2 to acetonyl peroxy radicals. Table 1, which will be discussed later, summarizes the most important reactions that must be taken into account. The impact of these processes on the PAN quantum yield under these conditions was explored with the help of computer simulations. Here we report PAN quantum yields observed in the experiments, the results of the computer calculations, and an evaluation of the experimental data to derive the branching ratio of reaction (3). In addition, information on the rate coefficient for the thermal decomposition of acetonyl peroxy nitrate was obtained.

Table 1. Reactions and rate constants[a] used in the computer simulations.

(P1)	$Cl_2 + h\nu \rightarrow Cl + Cl$	$3.3 \times 10^{-5}\ s^{-1}$
(P2)	$NO_2 + h\nu \rightarrow NO + O$	$3.8 \times 10^{-5}\ s^{-1}$
(P3)	$CH_3COCH_3 + h\nu \rightarrow \dot{C}H_3 + CH_3\dot{C}O$	$9.1 \times 10^{-9}\ s^{-1}$
(1)	$Cl + CH_3COCH_3 \rightarrow HCl + CH_3CO\dot{C}H_2$	2.1×10^{-12}
(2)	$CH_3CO\dot{C}H_2 + O_2 \rightarrow CH_3COCH_2OO\cdot$	7.5×10^{-11}
(3a)	$2\ CH_3COCH_2OO\cdot \rightarrow CH_3COCH_2OH + CH_3COCHO + O_2$	8.0×10^{-12} [b]
(3b)	$\rightarrow 2\ CH_3COCH_2O\cdot + O_2$	k_{3b}/k_3
(4)	$CH_3COCH_2O\cdot + O_2 \rightarrow CH_3COCHO + HO_2$	8.0×10^{-15}
(5)	$CH_3COCH_2O\cdot \rightarrow CH_3\dot{C}O + HCHO$	$5.0 \times 10^{7}\ s^{-1}$
(6)	$CH_3\dot{C}O + O_2 \rightarrow CH_3C(O)OO\cdot$	5.0×10^{-11}
(7)	$CH_3C(O)OO\cdot + NO_2 \rightleftharpoons CH_3C(O)OONO_2$	$8 \times 10^{-12}/5.5 \times 10^{-4}\ s^{-1}$
(8)	$CH_3COCH_2OO\cdot + NO \rightarrow CH_3COCH_2O\cdot + NO_2$	8.0×10^{-12}
(9)	$CH_3COCH_2OO\cdot + NO_2 \rightleftharpoons CH_3COCH_2OONO_2$	$6.4 \times 10^{-12}/k_{-9}$ [c]
(10)	$O + O_2 + M \rightarrow O_3 + M$	5.8×10^{-34}
(11)	$O_3 + NO_2 \rightarrow NO_3 + O_2$	3.2×10^{-17}
(12)	$NO_3 + NO_2 \rightleftharpoons N_2O_5$	$1.2 \times 10^{-12}/6.5 \times 10^{-2}\ s^{-1}$
(13)	$NO_3 + NO \rightarrow 2\ NO_2$	2.7×10^{-11}
(14)	$NO_3 + CH_3COCH_3 \rightarrow HNO_3 + CH_3CO\dot{C}H_2$	8.5×10^{-18}

[a] The units of rate coefficients are $cm^3\ molecule^{-1}\ s^{-1}$ unless otherwise noted. [b] Overall rate coefficient. [c] The rate coefficient k_{-9} for the reverse path of reaction (9) was treated as an adjustable parameter.

2. Experimental Section

The xenon lamp-monochromator setup was the same as that used previously in studying the photolysis of acetone [6]. A narrower monochromator slit width was applied in order to reduce the photolysis rate. The wavelength band was set to (330 ± 2) nm. A cylindrical quartz cuvette, 10 cm long and 1.8 cm i. d., served as the photolysis cell. The internal volume, including the inlet, was 29.93 cm^3. The radiation flux emerging from the monochromator exit slit and traversing the photolysis cell was $(3-4) \times 10^{14}$ photon s^{-1}. Rates for the individual photolytic processes were calculated from measured absorption cross sections for chlorine, nitrogen dioxide and acetone of 2.57×10^{-19}, 3.0×10^{-19} and $7.5 \times 10^{-22}\ cm^2$, respectively, at 330 nm. Average photodissociation rates are included in Table 1. They are based on a dissociation quantum yield for acetone of $\phi = 0.1$ at atmospheric pressure [6], and unity for the other two processes.

Gas mixtures were prepared by means of a suitable gas handling manifold. A typical gas mixture used in one series of experiments contained 1.05% acetone, 19.6% oxygen, 68.9 ppm Cl_2 and 14 ppm NO_2 in nitrogen. For such conditions the photolysis of Cl_2 followed by the reaction of chlorine atoms with acetone was the dominant process, whereas the photolysis of acetone as a source of acetyl peroxy radicals was almost negligible in comparison. The photodissociation rate of NO_2 was about 23% of that of Cl_2, which was close to 5.6×10^{10} molecule $cm^{-3}\ s^{-1}$.

In a second series of experiments, about 1 ppm of nitric oxide was deliberately added to the above mixture in order to assess the impact of NO on the system. Following preparation, each gas mixture was filled into the photolysis cell to a pressure of 103 kPa (765 torr), on average, which resulted in the concentrations: $[Cl_2] = 1.7 \times 10^{15}$, [acetone] = 2.65×10^{17}, $[NO_2] = 3.45 \times 10^{14}$, $[O_2] = 4.85 \times 10^{18}$, $[NO] \approx 2.5 \times 10^{13}$ molecule cm^{-3}.

PAN was determined by gas chromatography immediately after irradiation of the gas mixture. Generally, less than 5 min elapsed between terminating the photolysis and transferring a sample from the photolysis cell into the carrier gas flow of the gas chromatograph. The instrument combined a 50 cm long, 3.7 mm i. d. glass column, packed with 10% Carbowax 600 on Chromosorb, with a home-built NO-O_3 chemiluminescence detector. The details, including a correction for losses of PAN on the column, have been described in [6]. In the present case, the aggressiveness of chlorine on the column made it necessary to replace the column more frequently than usual.

3. Calculations

The FACSIMILE computer code [8] was used. The salient features of the chemical mechanism employed in the simulations are presented in Table 1. This is a condensed list of a more extensive set of reactions that had been used previously [6] to describe the photodecomposition of acetone in the presence of NO_2. The required additions were reactions (P1) and (1) describing the production of chlorine atoms and their reaction with acetone, the formation of acetonyl peroxy nitrate in reaction (9), and, finally, hydrogen abstraction from acetone by the nitrate radical, reaction (14). Reactions of chlorine atoms with products resulting from reaction (3), primarily hydroxy acetone, methyl glyoxal and formaldehyde, were included in the full scheme with rate coefficients taken from Jenkin *et al.* [3]. These reactions were found to have a negligible effect owing to the high acetone/product concentration ratios in the experiments. The formation of acetonyl peroxy nitrate, reaction (9), has been studied by Sehested *et al.* [7], who subjected a mixture of acetone, NO_2 and SF_6 in air to pulse radiolysis and determined the forward rate coefficient from the decay of NO_2. The reverse rate coefficient was derived indirectly by means of computer simulation of the observed thermal decay of acetonyl peroxy nitrate in the presence of excess NO_2. The rate coefficients were $k_9 = 6.4 \times 10^{-12}$ cm^3 $molecule^{-1}$ s^{-1} for the forward reaction and $k_{-9} = 3.0$ s^{-1} for the reverse reaction. We have employed the forward rate constant, which was determined in a direct manner, but treated the rate of the reverse reaction as an adjustable parameter, because the results of our experiments suggested that the decomposition rate is slightly faster. Reaction (14) also was not considered previously. It was added because under our experimental conditions, NO_3 (plus N_2O_5) and NO are major products arising from NO_2 photodissociation. The rate coefficient for reaction (14) is small [9], yet owing to the high concentration of acetone it was not clear whether the reaction might become important at longer irradiation times, when the concentration of NO, with which NO_3 reacts initially, has declined to low values due to consumption in reaction (8).

4. Results

PAN was the only product detected. Acetonyl peroxy nitrate is not expected to survive analysis by gas chromatography, and there was no indication for its presence in the chromatograms. Figure 1 shows PAN quantum yields as a function of irradiation time. Quantum yields refer to the photodissociation of chlorine. They were calculated from the amount of PAN produced and the effective radiation dose. Each point in Fig. 1 represents an average of at least three independent determinations. The vertical bars indicate the standard deviation (2σ).

In the experiments with NO added to the gas mixtures, the PAN quantum yield is initially 1.95 ± 0.15, on average. Approximately 80 s after starting the irradiation the quantum yield decreases and reaches a value of 1.28 ± 0.07 after 720 s. Because two chlorine

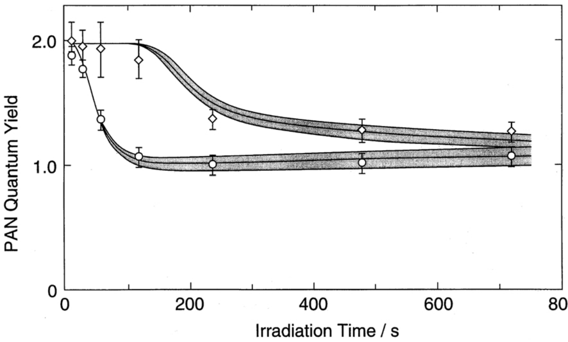

Fig. 1. PAN quantum yield as a function of irradiation time. Symbols: diamonds, experiments with deliberate NO addition; circles, experiments without NO addition (initial high values indicate NO impurity). The solid lines and the shaded areas are results of computer simulations that are described in the text.

atoms are produced when chlorine is photolysed, the sequence of reactions (1) – (8) in Table 1 is expected to produce a PAN quantum yield of nearly two, provided the acetonoxy radical undergoes primarily the decomposition reaction (5). The measured initial value is in accord with this expectation. The observation that the quantum yield eventually declines must then be due to the consumption of NO in reaction (8) and the increasing importance of reaction (3) in the mechanism. As Fig. 1 shows, the experiments performed without adding NO to the gas mixtures also gave an initially high PAN quantum yield, 1.89 ± 0.03 after 20 s photolysis time. This result was unexpected. However, the quantum yield declines rapidly toward values near unity, which is reached after 200 s and is maintained thereafter. The behavior suggests that some NO was initially present, occurring as an impurity in the gas mixture. The computer simulations demonstrated that the effect of NO_2 photolysis on the PAN quantum yield is relatively minor, especially during the initial stage of photolysis. The amounts of NO required to reproduce the experimental results without deliberate NO addition were found to be $(2-3) \times 10^{12}$ molecule cm^{-3}. This is less than 1% of NO_2 and may well have been present as an unintentional impurity.

The computer simulations included a 5 min dark period following irradiation to make allowance for the decomposition of acetonyl peroxy nitrate during the time required to transfer the sample for analysis. At short irradiation times, when some NO remains present at the end of the irradiation period, acetonyl peroxy nitrate decays rapidly during the dark period due to reaction (8). After 100 – 200 s of irradiation the concentration of NO declines to low values ($\sim 2 \times 10^{10}$ molecule cm^{-3}), which are maintained by NO_2 photolysis. The decay of acetonyl peroxy nitrate then slows down, and the calculations demonstrate that the partial conversion of acetonyl peroxy nitrate subsequent to photolysis raises the PAN quantum yield by approximately 10%. Increasing the dark period to 15 min enhances the PAN quantum yield fairly little beyond that reached after 5 min.

The computer calculations clearly showed that our experimental data are inadequately simulated by the values for k_{3b}/k_3 and k_{-9} reported by Bridier *et al.* [2] and Sehested *et al.* [7], respectively. Therefore, the branching ratio k_{3b}/k_3 and the rate constant k_{-9} were treated as adjustable parameters. By readjusting the values in a stepwise manner, the calculated and observed PAN quantum yields could be brought into agreement, for both series of experiments (i.e. with and without addition of NO). The best approximation was achieved with $k_{3b}/k_3 = 0.50$ and $k_{-9} = 10\ s^{-1}$. The PAN quantum yields calculated with these values are shown in Fig. 1 by the solid lines. The shaded areas surrounding both curves represent the range $0.45 < k_{3b}/k_3 < 0.55$ and $7 < k_{-9} < 13$. Further calculations, in which the formation of acetonyl peroxy nitrate was deleted from the mechanism, led to a branching coefficient $k_{3b}/k_3 = 0.45 \pm 0.05$, slightly lower than the value derived with the full mechanism. In this case, however, the upward trend of the PAN quantum yield observed at longer irradiation times (see Fig. 1) could not be reproduced.

The effect caused by the reaction of nitrate radicals with acetone turned out to be surprisingly small on the time scale of the experiments. The reason is that the NO_3 radicals arising from the photolysis of NO_2 are stored and accumulate largely in the form of N_2O_5. While the equilibrium of reaction (12) is rapidly established, the high ratio $[N_2O_5]/[NO_3] = (k_{12}/k_{-12})[NO_2] \approx 6 \times 10^3$ keeps the concentration of NO_3 at a low level. The radicals are slowly released subsequent to irradiation, and they contribute via reaction (14) to the post-photolysis rise of the PAN quantum yield. The calculations indicate that the concentration of N_2O_5 reached after 700 s would ultimately contribute about 9% to the PAN quantum yield observed, but the time constant for the decay of N_2O_5 due to reaction (14) is 40 min, much longer than the time scale of the present experiments.

5. Discussion

The aim of the present study was to determine the branching ratio of reaction (3) from the yield of PAN formed in the reaction of acetyl peroxy radicals with NO_2, where the acetyl peroxy radicals are formed by decomposition of acetonoxy radicals produced in reaction (3b). The major assumptions are that this is the only source of acetyl peroxy in the system and that other reactions of acetonoxy are insignificant. As outlined in the introduction, the first of these assumptions is not fully met, due to the effects of NO_2 photolysis as well as a temporary storage of acetonyl peroxy in the form of acetonyl peroxy nitrate. These effects were explored by computer simulations. The time-dependent PAN quantum yields observed here suggest that the decay constant for acetonyl peroxy nitrate is $k_{-9} = (10 \pm 3)\ s^{-1}$, about three times greater than that reported by Sehested *et al.* [7]. The disagreement is not considered serious, in view of the difficulties experienced in determining the coefficient from the decay of acetonyl peroxy nitrate. Our calculations show that at the end of the observation period most acetonyl peroxy nitrate has decayed to less than 15% of that of PAN. The rise of the PAN quantum yield caused by the final decay lies within the experimental error. The calculations further show that the upward trend of the PAN quantum yield made evident in Fig. 1 at longer irradiation times is caused solely by the decay of acetonyl peroxy nitrate, and not by the formation of additional acetonyl peroxy radicals from the reaction of NO_3 with acetone.

The branching ratio $k_{3b}/k_3 = 0.50 \pm 0.05$ obtained here is appreciably lower than that derived by Bridier *et al.* [2], 0.75 ± 0.1. The value appears to be independent of the decay constant chosen for acetonyl peroxy nitrate. The upper limit that would still barely agree with our experimental data is$k_{3b}/k_3 = 0.6$, but even this value lies below the range 0.65 – 0.85 reported previously. The experiments of Bridier *et al.* did not involve NO_x. As a consequence the acetyl peroxy radicals undergo subsequent reactions that make the chemical system more complex and give rise to greater uncertainties compared with the present system, in which the acetyl peroxy radicals are stabilized as PAN.

The presence of an NO impurity in our gas mixtures prevented us from observing the PAN yield from reaction (3b) during the initial phase of irradiation. Information about k_{-9} and k_{3b}/k_3 is obtained primarily from the rate of PAN formation at times when the concentration of NO has declined to low values, that is, 200 s after starting experiments in which NO was deliberately added, and 100 s after starting experiments without NO addition. Even at later times some NO is present due to the photolysis of NO_2. In the dark period following irradiation the remaining NO is consumed by reaction with acetonyl peroxy, but the calculations show that the amount of PAN resulting from this process is insignificant compared to that arising from the thermal decay of acetonyl peroxy nitrate. During irradiation, according to our analysis, the concentration of acetonyl peroxy radicals generated per second from the photodissociation of chlorine is approximately 1.12×10^{11} molecule cm^{-3}, whereas that destroyed by NO arising from NO_2 photolysis is 1.29×10^{10} molecule cm^{-3} at the most. This corresponds to approximately 11% of the acetonyl peroxy radicals that are converted directly to acetyl peroxy, and to 20% of PAN produced from reactions (3b) and (8) combined. The photolysis of NO_2 leads also to the formation of NO_3, which reacts with acetone to produce acetonyl peroxy. The contribution of this process, however, is negligible on the time scale of our experiments, because most of the NO_3 is tied up as N_2O_5. Thus, the main effect of NO_2 photolysis under our experimental conditions is to generate about ten percent more PAN than one would observe if NO were entirely absent.

[1] R. A. Cox, J. Munk, O. J. Nielsen, P. Pagsberg, and E. Ratajczak, Chem. Phys. Lett. **173**, 206 (1990).

[2] I. Bridier, B. Veyret, R. Lesclaux, and M. E. Jenkin, J. Chem. Soc. Faraday Trans. **89**, 2993 (1993).

[3] M. E. Jenkin, R. A. Cox, M. Emrich, and G. K. Moortgat, J. Chem. Soc. Faraday Trans. **89**, 2983 (1993).

[4] J. J. Orlando, G. S. Tyndall, L. Vereecken, and J. Peeters, J. Phys. Chem. A **104**, 11578 (2000).

[5] P. Warneck and T. Zerbach, Environ. Sci. Technol. **26**, 74 (1992).

[6] M. Emrich and P. Warneck, J. Phys. Chem. A **104**, 9436 (2000).

[7] J. Sehested, L. K. Christensen, O. J. Nielsen, M. Bilde, T. J. Wallington, W. F. Schneider, J. J. Orlando, and G. S. Tyndall, Int. J. Chem. Kinet. **30**, 475 (1998).

[8] A. R. Curtis and W. P. Sweetenham, AERE Harwell Report 12805 (1988).

[9] R. P. Wayne, I. Barnes, P. Biggs, J. P. Burrows, C. E. Canosa-Mas, J. Hjorth, G. Le Bras, G. K. Moortgat, D. Perner, G. Poulet, G. Restelli, and H. Sidebottom, Atmos. Environ. **25A**, 1 (1991).